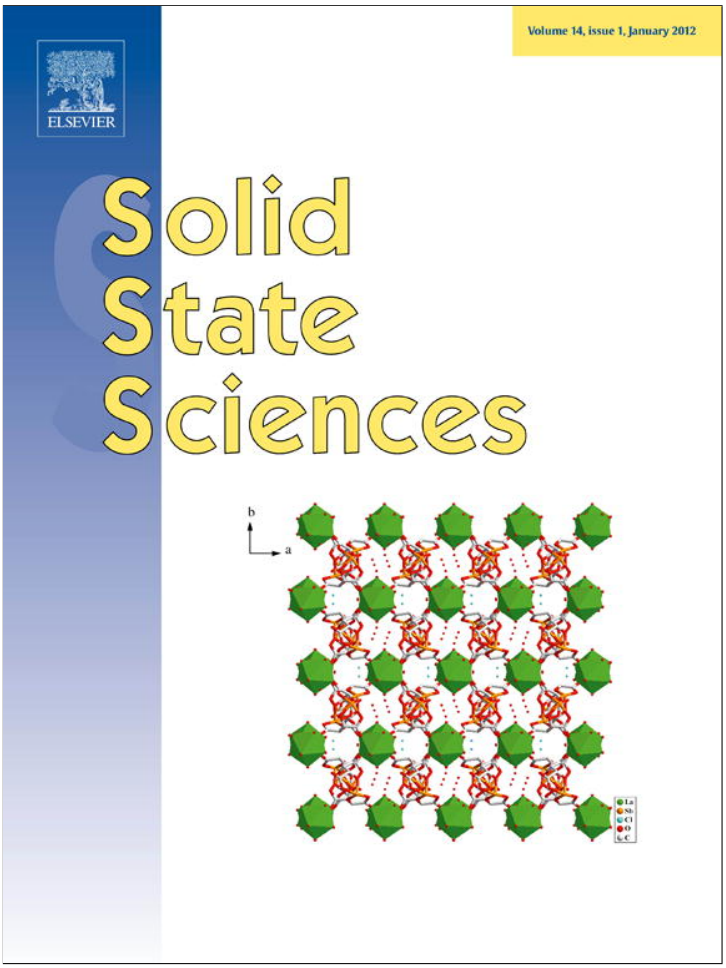

Solid State Sciences 20 (2013) 97–102

Contents lists available at SciVerse ScienceDirect

Solid State Sciences

journal homepage: www.elsevier.com/locate/ssscie

Problems with the thermogravimetric determination of oxygen stoichiometries in pure and rare-earth substituted La_2RuO_5

S. Riegg [a], T. Müller [b], S.G. Ebbinghaus [b,*]

[a] Experimental Physics V, Center for Electronic Correlations and Magnetism, University of Augsburg, D-86159 Augsburg, Germany
[b] Solid State Chemistry, Martin-Luther University Halle-Wittenberg, D-06099 Halle, Germany

ARTICLE INFO

Article history:
Received 4 October 2012
Received in revised form
3 March 2013
Accepted 19 March 2013
Available online 2 April 2013

Dedicated to Prof. Dr. Armin Reller on the occasion of his 60th birthday.

Keywords:
La_2RuO_5
Ruthenates
Thermogravimetry
EXAFS
X-ray absorption spectroscopy
Oxygen stoichiometry

ABSTRACT

The oxygen stoichiometries of pure and rare-earth substituted La_2RuO_5 have been investigated by thermogravimetry (TG) in reducing atmosphere. Assuming that the observed total weight loss is caused by the reduction of Ru^{4+} to Ru-metal, remarkable oxygen deficiencies were calculated. These would correspond to ruthenium oxidation states significantly lower than the ones experimentally observed by XANES. To explain this discrepancy we investigated the reduction products by X-ray absorption spectroscopy (XAS). EXAFS measurements at the Ru–K edge revealed the presence of an X-ray amorphous ruthenium oxide, indicating an incomplete reduction. The apparent oxygen deficiencies obtained for pure and rare-earth substituted samples correlate with the amount of remaining ruthenium oxide. The presence of a ruthenium oxide species was furthermore verified by Ru–L_{III} XANES investigations. Our results show that the determination of oxygen contents by thermogravimetry might fail even for the easily reducable nobel metal oxides and therefore has to be applied with caution if the reaction products cannot be identified unambiguously.

1. Introduction

The thermogravimetric determination of oxygen contents of binary or complex oxides is a versatile and popular method applied since many years [1,2]. Thermogravimetric oxygen determination is especially useful for oxides of nobel metals since these can easily be reduced to the corresponding metals in e.g. forming gas (H_2/N_2 or H_2/Ar mixtures). Specifically for ruthenates this method has been used in many investigations leading to highly interesting results [3]. For example, Reller et al. found that for $Sr_2Ru_{1-x}Ti_xO_4$ the reduction temperature increases with the Ti content due to the stabilization of the crystal lattice by the reduction-stable titanium, a phenomenon denoted as shielding effect [4]. For $La_{2-x}Sr_xCu_{1-y}Ru_yO_{4-\delta}$ it was found thermogravimetrically that the oxygen deficit δ varies systematically with x and y according to $\delta \approx x/2 - y - 0.2$ for $x > 2y + 0.4$ [5]. EXAFS and XANES investigations later showed that the oxygen vacancies exclusively affect the copper ions, while ruthenium remains octahedrally coordinated [6]. For the hexagonal ruthenates $(La,Sr)_4RuO_{7+\delta}$ the reduction in forming gas revealed an oxygen excess of $\delta \cong 1/3$ due to the presence of peroxide ions [7].

Thermogravimetry is neither restricted to (complete) reductions nor to the late transition metals. As an example, Wurr and Reller [8] showed that various manganese oxides can partly be reduced to MnO and Lichtenberg and Reller [9] determined the oxygen content of layered $La_{n+1}Ti_{n+1}O_{3n+5}$ by thermogravimetric oxidation leading to $La_2Ti_2O_7$.

While these examples show the high potential of the thermogravimetric oxygen determination, in the following we discuss a compound for which this method fails although at first sight one would not expect any problems.

La_2RuO_5 has a layered crystal structure with $LaRuO_4$ perovskite-like layers and buckled LaO layers alternating along the a-axis as depicted in Fig. 1 and described in more detail in Refs. [10,11]. The unsubstituted La_2RuO_5 shows a phase transition at roughly 160 K, which affects structure, magnetic properties and electrical conductivity [12,13]. The high temperature (ht-) phase is characterized by a monoclinic symmetry (space group $P2_1/c$, no. 14), a paramagnetic behavior in accordance with the $S = 1$ moments of the Ru^{4+} ions and a band gap of approximately 0.15 eV [12]. In contrast, the low temperature (lt-) phase has a triclinic symmetry (space group $P\bar{1}$, no. 2), the magnetic susceptibility is strongly reduced to

* Corresponding author. Tel.: +49 345 55 25870.
E-mail address: stefan.ebbinghaus@chemie.uni-halle.de (S.G. Ebbinghaus).

1293-2558/$ – see front matter © 2013 Elsevier Masson SAS. All rights reserved.
http://dx.doi.org/10.1016/j.solidstatesciences.2013.03.018

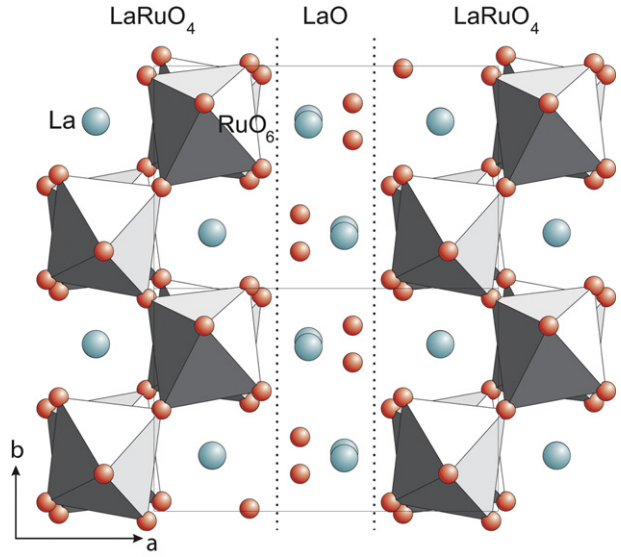

Fig. 1. Crystal structure of La_2RuO_5 viewed along the *c*-axis. La is represented by large turquoise spheres, oxygen by small red spheres and the RuO_6 octahedra are colored gray. The alternating layering of LaO and $LaRuO_4$ along the *a*-axis is indicated by dotted lines. (For interpretation of the references to color in this figure legend, the reader is referred to the web version of this article.)

roughly 10^{-4} emu/mol and the conduction band gap increases to 0.21 eV [12]. During this transition the almost regular arrangement of the Ru centers is transformed to a distorted structure with significantly alternating Ru–Ru distances, which induces the formation of antiferromagnetic spin dimers in a non-magnetic singlet ground state [14]. This finding is supported by density functional theory calculations applying different approaches for mapping the electron density [15–17].

Recently, we managed to synthesize rare-earth substituted La_2RuO_5 ($La_{2-x}Ln_xRuO_5$: Ln = Pr, Nd, Sm, Gd, Dy) powder samples by a soft chemistry reaction based on the thermal decomposition of citric acid stabilized precursors [18,19]. The preferred incorporation of the smaller rare-earth ions in the LaO-layers shifts the phase transition to lower temperatures with increasing substitution level but preserves the formation of the Ru-spin dimers [19–21].

The physical properties of oxides are often strongly affected by their oxygen stoichiometry, especially by oxygen defects. The perhaps most prominent example is the suppression of superconductivity in $YBa_2Cu_3O_{7-\delta}$ with decreasing oxygen content. Thus the question arose, whether the observed changes in the phase transition of substituted La_2RuO_5 might be caused by oxygen non-stoichiometries. Therefore, the oxygen contents of the pure and substituted La_2RuO_5 samples were determined by thermogravimetry (TG) in reducing atmosphere. The reaction products after TG measurement were investigated by powder X-ray diffraction (XRD) and by X-ray absorption spectroscopy (XAS) at the Ru–K and Ru–L_{III} absorption edges. The obtained rather surprising results revealed an incomplete reduction leading to incorrect values of the thermogravimetrically derived oxygen contents.

2. Experimental

Polycrystalline samples of (substituted) La_2RuO_5 were prepared as described in detail in Refs. [18,19]. For the rare-earth incorporation, ethanolic solutions of stoichiometric amounts of $La(NO_3)_3 \times 6H_2O$, $Ln(NO_3)_3 \times 6H_2O$, ruthenium–acetylacetonate (Ru–AcAc) with a threefold excess of citric acid as complexing agent were dried, pyrolyzed at 600 °C and calcined at 1175 °C for at least 96 h. Using the water soluble Ru-agent ruthenium–nitrosyleacetate (Ru–NOAc) an additional sample of La_2RuO_5 was obtained from an aqueous precursor [22]. The same heat treatment as for the Ru–AcAc route was applied.

For the thermogravimetric measurements a TA-Instruments 2950 thermobalance was used. Approximately 50 mg of sample powder were heated in alumina crucibles with a constant rate of 10 K/min from room temperature to 950°. This temperature was held for 15 min. During the measurement a gas flow of 75 ml/min forming gas (5% H_2 in N_2) was applied. An additional flow of 25 ml/min Ar passed through the balance as protecting gas. A baseline measurement was performed using roughly 40 mg of dry Al_2O_3 and applied for the buoyancy correction.

Powder X-ray diffraction patterns were recorded on a Bruker D8 Advance Bragg–Brentano diffractometer in θ/θ-geometry with Cu-K_α radiation. A one-dimensional silicon strip detector (LynxEye) was used. Measurements were carried out in the angular range $10° \leq 2\theta \leq 60°$ with a step size of 0.01° and a counting time of 1 s per data point.

Ru–K EXAFS spectra were measured in transmission mode at the beamline X1 of HASYLAB at DESY. Approximately 100 mg of the sample powders were mixed with 25 mg of cellulose and pressed into pellets of 13 mm diameter. A Si(311) double monochromator was used and the incoming beam was detuned to 70% of the maximum intensity to suppress higher harmonics. The pre-edge region 21.900–22.000 keV was measured in energy steps of 2 eV for background determination. In the vicinity of the Ru–K absorption edge (Ru–K: 22.117 keV) [23], i.e. between 22.000 and 22.160 keV steps of 1 eV and an integration time per data point of 2 s was used. The EXAFS range between 22.160 and 24.000 keV was measured in equidistant steps in *k*-space of 0.05 $Å^{-1}$. The integration time per data point was increased linearly. The spectra were energy-calibrated against the first inflection point of a simultaneously recorded Ru-metal foil.

Data evaluation was performed using the program VIPER [24]. The pre-edge background μ_b was determined by fitting the range 21.900–22.050 keV with a polynomial function with coefficients x^{-3} and x^1. The atomic absorption coefficient μ_0 was obtained from a smoothing spline fit of the post-edge region. For the conversion from energy to *k*-space the threshold energy E_0 was calculated from the maximum of the first derivative of the normalized spectra. The finally obtained $\chi(k)$ curves were fit using the program WinXAS [25]. After weighing with k^2, a Bessel-window was applied and the spectra were Fourier-transformed to obtain the modified radial distribution functions (mRDFs). Theoretical scattering amplitudes and phase shifts for the mRDF fits were modeled utilizing FEFF8 [26].

Additional XANES spectra at the Ru–L_{III} edge (E = 2.838 keV) [23] were recorded at beamline A1 of HASYLAB. The sample powders and the references (Ru-metal and RuO_2 powder) were stuck to adhesive tape. Spectra were obtained in transmission mode, energy calibrated to the first inflection point of the Ru-metal reference and normalized to the first minimum above the white lines at the absorption edge.

3. Results and discussion

The relative weight changes for three La_2RuO_5 samples synthesized by different reaction routes are depicted in Fig. 2. The sample notation refers to the applied Ru-agent in the preparation as described in Section 2. For comparison, a sample prepared by the classical solid state reaction route was also measured. Two distinct and well-separated weight reduction steps of approximately 2% and 5% are observed for all samples. The first reduction step is completed at roughly 550 °C and results in a stable intermediate state, as already observed by Benčan et al. [27]. The inflection point

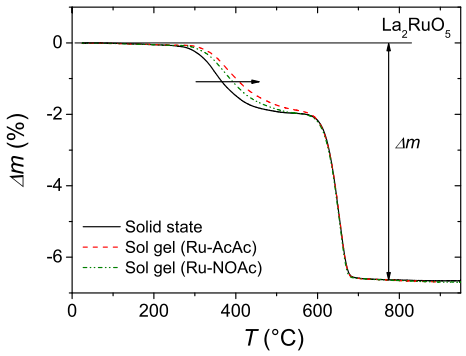

Fig. 2. Relative weight change for La_2RuO_5 samples synthesized by different reaction routes and varying calcination times.

of the first reduction step differs by roughly 50 °C. In contrast, the second reduction step is very similar for all three samples and occurs in a narrow temperature range of roughly 620–680 °C. At 700 °C the reduction is completed and the final weight loss is apparently identical for all three samples.

The obtained total weight losses of 6.64–6.70% are slightly smaller than the value of 6.9% reported in literature [27]. Assuming that La_2RuO_5 is decomposed to La_2O_3 and metallic Ru during the reaction, a theoretical weight loss of 6.97% is calculated for two released oxygen atoms ($z = 2$) according to the reaction:

$$La_2RuO_{3+z} + z\cdot H_2(g) \rightarrow La_2O_3 + Ru + z\cdot H_2O(\uparrow). \quad (1)$$

From the experimentally found weight losses the oxygen content z was calculated using:

$$z = \left(\frac{1}{1-\Delta m} - 1\right)\cdot\frac{M_f}{M(O)}, \quad (2)$$

where Δm denotes the measured relative weight loss determined in the temperature range 110 °C and 755 °C, $M(O)$ is the molecular mass of oxygen and M_f is sum of the molecular masses of the non-volatile products of the reaction (Eq. (1)). The values determined for Δm and the corresponding oxygen contents for all investigated samples are given in Table 1. For convenience we also listed (apparent) deficiencies $\delta = 5 - (3 + z)$. It is striking that for all three samples of La_2RuO_5 significant deficiencies in the range of $\delta \approx 0.09$ were found. Such high values cannot be explained by instrumental errors. From experience we estimate a general reproducibility of roughly 10 μg for the measurements. Taking into account an additional uncertainty of 10–20 μg for the baseline correction, a standard deviation of 0.03 can be estimated for the oxygen content.

Table 1
Relative weight losses and oxygen contents of selected pure and substituted La_2RuO_5 samples. Estimated standard deviations are 0.05 for Δm and 0.03 for the oxygen contents/deficiencies.

Compound	Δm (%)	Oxygen content	Oxygen deficit δ
La_2RuO_5 (solid state)	6.64	4.90	0.10
La_2RuO_5 (sol–gel Ru–AcAc)	6.69	4.91	0.09
La_2RuO_5 (sol–gel Ru–NOAc)	6.70	4.92	0.09
$La_{1.75}Pr_{0.25}RuO_5$	6.85	4.93	0.07
$La_{1.25}Pr_{0.75}RuO_5$	6.84	4.94	0.06
$La_{1.5}Nd_{0.5}RuO_5$	6.70	4.93	0.07
$La_{1.6}Sm_{0.4}RuO_5$	6.65	4.92	0.08
$La_{1.7}Gd_{0.3}RuO_5$	6.53	4.89	0.11
$La_{1.8}Dy_{0.2}RuO_5$	6.44	4.86	0.14

The values listed in Table 1 are well above the 2σ-limit for most of the samples.

In Fig. 3 the thermogravimetric results for selected $La_{2-x}Ln_xRuO_5$ compounds are shown. The rare-earth substitution does not change the absolute shape of the curves, i.e. the two separate steps are still observable. The relative weight losses change depending on the atomic weight of the lanthanide and the substitution level. Due to the rare-earth substitution a slightly modified reaction equation has to be used to calculate the oxygen content:

$$La_{2-x}Ln_xRuO_{3+z} + z\cdot H_2(g) \rightarrow (2-x)\cdot La_2O_3 + x\cdot Ln_2O_3 + Ru + z\cdot H_2O(\uparrow). \quad (3)$$

The M_f used in Eq. (2) changes according to the content of Ln_2O_3. The oxygen contents/deficiencies for $La_{2-x}Ln_xRuO_5$ calculated using Eq. (2) are also listed in Table 1. The obtained deficiencies range between 0.06 and 0.14 (Table 1), and thus, are significantly larger than the calculated error of ±0.03.

The reduction products were examined by powder XRD. In Fig. 4 the pattern of La_2RuO_5 after the TG measurement is shown. All peaks can be identified as α-La_2O_3 and $La(OH)_3$, which is formed by the reaction of the hygroscopic La_2O_3 with air moisture. Strikingly, the expected Ru-metal was not detected for any of the samples. A similar finding was reported by Benčan et al. [27], where the Ru-metal was not observed in the XRD patterns either, but was identified by selected area electron diffraction. These authors explained the absence of Ru-metal diffraction peaks by very small particle sizes.

This interpretation is not convincing, because for all other ruthenium oxides we investigated to date, Ru-metal was clearly detected by XRD. In Fig. 4b the pattern of the ruthenate $NdSr_3RuO_{7+\delta}$ after reduction (same reaction conditions as for La_2RuO_5) is shown as one example. The Ru-metal peaks are clearly visible. The other peaks can be explicitly ascribed to Nd_2O_3 and $Sr(OH)_2$, which are the other expected reaction products.

For the (substituted) La_2RuO_5 samples the oxidation states of Ru and the substituting elements were determined by X-ray absorption near edge structure (XANES) investigations and magnetic susceptibility measurements. For all compounds a Ru-valence of +4 was found [19,21]. The calculated oxygen deficiencies according to Table 1 correspond to oxidation states well below +4 for ruthenium, in clear contradiction to the results of the XAS and magnetic measurements. Furthermore, neutron diffraction experiments gave no indications for vacancies on the oxygen sites either [11,19]. The absence of Ru-metal peaks in the XRD is a hint that this apparent contradiction might be caused by an incomplete reaction.

To gain a better insight in the nature of the ruthenium-related reduction products, X-ray absorption spectroscopy measurements at the Ru–L_{III} and Ru–K edges were carried out. XAS is highly

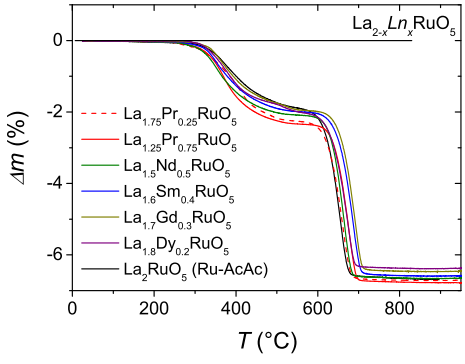

Fig. 3. Relative weight change for selected $La_{2-x}Ln_xRuO_5$ samples.

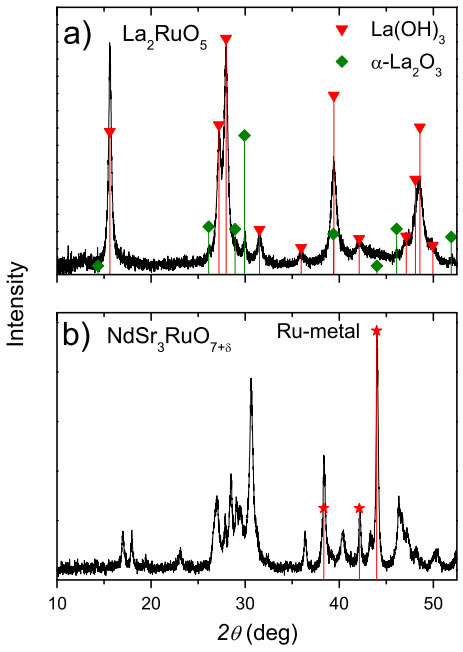

Fig. 4. XRD patterns of a) La_2RuO_5 and b) $NdSr_3RuO_{7+\delta}$ after thermogravimetric measurement in reducing atmosphere. a) The markers indicate the 2θ-values and intensities of $La(OH)_3$ (PDF 036-1481) (red) and α-La_2O_3 (PDF 071-4953) (green). b) The red markers represent the 2θ-values and intensities of Ru-metal (PDF 065-1863). (For interpretation of the references to color in this figure legend, the reader is referred to the web version of this article.)

element specific and not restricted to crystalline samples. For these reasons (possibly amorphous) Ru compounds can be investigated while by-products like $Ln(OH)_3$ do not interfere.

The normalized XANES spectra at the Ru–L_{III} absorption edge are shown in Fig. 5. The so-called "white line" observed at the Ru–L_{III} edge is caused by transitions from the $2P_{3/2}$ core state to unoccupied states with predominantly 4*d* character. The intensity, fine structure, and energy position of the white line is affected by several parameters, like the number of available states (which reflects the oxidation state), coordination geometry and hybridization of the Ru-4*d* orbitals with ligand orbitals. The Ru-metal reference shows a single, broad absorption peak with a rather low intensity. On the other hand, RuO_2 provides the typical edge shape of ruthenium-based oxides with two very intense white lines. These two white lines correspond to excitations into the $4d$-t_{2g} and e_g levels of Ru in an octahedral oxygen coordination [28]. The same structure of the white lines was also observed for the original (i.e. not reduced) La_2RuO_5 [21]. The XANES spectra of the reduced

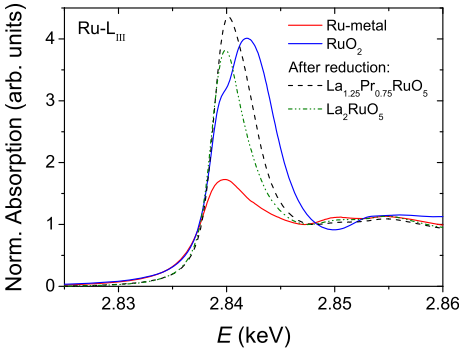

Fig. 5. Normalized Ru–L_{III} absorption spectra of reduced $La_{1.25}Pr_{0.75}RuO_5$ (at 950 °C) and La_2RuO_5 (at 1100 °C) in comparison with the references Ru-metal and RuO_2.

samples are clearly different from the one of ruthenium metal, indicating that the reduction is not fully completed. It has to be noted that the reduction products of other ruthenium oxides like RuO_2 show XANES spectra that are identical with the Ru-metal reference. Thus the reduction behavior of (substituted) La_2RuO_5 is obviously different from the ones of other ruthenates. On the other hand, the XANES spectra of the reduced La_2RuO_5 samples also show clear differences compared to "normal" ruthenium-based oxides as shown e.g. in Refs. [29–32]. An obvious difference is the appearance of only one intense peak for the reduced samples. This peak indicates the presence of some bonded oxygen, i.e. the hybridization of Ru-4*d* and O-2*p* orbitals, but only in such small amounts that a splitting of the Ru-*d* orbitals into sets of different energy does not occur. For the different samples the peak exhibits a slightly different shape depending on the final temperature of the TG measurement. The pure La_2RuO_5, which was reduced up to 1100 °C (dash dot line), shows a narrower and smaller peak compared to the rare-earth substituted samples (dashed line) and the other unsubstituted La_2RuO_5, which were only reacted to 950 °C. The peak maxima of the Ru-metal and the La_2RuO_5 sample are in good agreement, whereas the maximum for the other samples is slightly shifted to higher energies by roughly 0.1 eV reflecting a small valence shift effect. This is also a sign of traces of oxidized Ru remaining in the TG reacted samples.

Considering the Ru–L_{III} absorption spectra, a quantitative analysis of a correlation between δ and the peak intensity was not possible, therefore additional Ru–K EXAFS spectra were recorded and analyzed.

From the Ru–K absorption spectra of selected samples the corresponding mRDFs were obtained by Fourier-transformation of the k^2-weighted EXAFS regions. They are depicted in the left frame of Fig. 6 together with the Ru-metal reference. For better comparability the mRDFs were normalized to the maximum of the main peak at roughly 2.2 Å. In the mRDF of the Ru-metal four distinct peaks at approximately 2.2 Å, 3.5 Å, 4.3 Å, and 5 Å are observed. The shown pattern is typical for metals with (hexagonal or cubic) close packing. These four peaks were also found for the reduction products of the (substituted) La_2RuO_5 samples, indicating that a reduction actually took place. Interestingly, for the reduced samples an additional peak at approximately 1.5 Å was found. This peak at the left side of the most intense peak, which corresponds to the first Ru-coordination shell in the metal, was only found for the reduced samples of La_2RuO_5-related compounds. The distance of 1.5 Å from the X-ray absorbing atom is typical for the Ru–O bond length taking into account that due to phase shifts during the absorption/backscattering process the interatomic distances seen in the mRDFs are systematically too small. In fact, the same peak distance of roughly 1.5 Å was found for all ruthenium oxides including e.g. La_2RuO_5 or RuO_2, and is a clear proof that a small fraction of oxidized ruthenium is preserved in the reduced samples after the TG treatment.

From Fig. 6 and Table 1 it is obvious that the peak intensity correlates with the obtained oxygen deficiency δ. For a quantitative analysis the peak areas were determined to study this correlation in detail. For this, the first coordination peak of the Ru-metal mRDF was fit to obtain a smooth, well-defined reference curve, which can be subtracted from the other samples' mRDFs. In this fit two Ru backscattering paths were used reflecting the two slightly distinct nearest-neighbor sites of the hexagonal lattice. The corresponding amplitudes and phase shifts were modeled by FEFF8. The distances of the shells amounted to 2.64(1) Å (Ru1) and 2.71(1) Å (Ru2). A fixed degeneracy of $N = 6$ for both backscattering paths was used according to the hexagonal close packing. In addition, identical Debye–Waller factors $\sigma^2 = 0.0033(1)$ Å^2 were used. The excellent agreement of the fit is shown in the right frame of Fig. 6. The fit

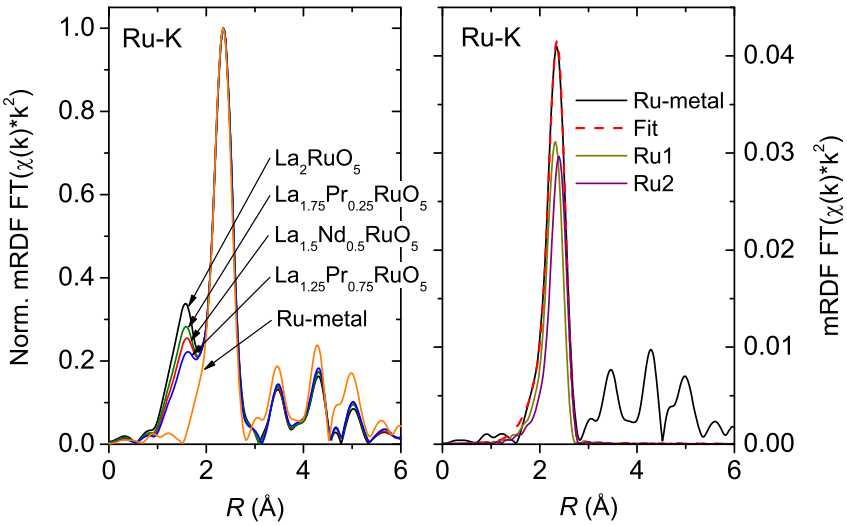

Fig. 6. Left: normalized mRDF obtained from the Ru–K EXAFS spectra of selected $La_{2-x}Ln_xRuO_5$ samples. Right: fit of the first two Ru-coordination shells for the Ru-metal reference.

curve was subtracted from the mRDFs of the reduced samples leading to the residuals shown in the left frame of Fig. 7.

The Ru–O related peaks were integrated between the shown markers to obtain numerical values for the peak intensities. These values are drawn vs. the corresponding oxygen deficits δ (from Table 1) in the right frame of Fig. 7. The Ru-metal sample was taken to have a zero peak area and $\delta = 0$. It is clearly visible that the peak areas show a linear correlation to the (apparent) oxygen deficits as indicated by the red dashed line, which represents a linear fit.

The linear correlation of δ and the Ru–O peak area illustratively reflects the incomplete reduction of pure and rare-earth substituted La_2RuO_5 samples resulting in a small fraction of remaining oxidized Ru. One might assume that the applied reduction temperature of 950 °C is not sufficient to obtain a complete reduction. For this reason we performed additional reductions on a Netzsch STA 409 thermobalance up to a temperature of 1100 °C. Even at this much higher temperature the reduction remained incomplete as deduced from the weight loss of 6.81% related to an (apparent) oxygen deficiency of $\delta = 0.05$. The fact that δ was found to be smaller than for the samples heated to only 950 °C but neither an additional reduction step nor a slow continuous weight loss were observed indicates that the reduction process becomes very slow at temperatures above ca. 800 °C. Furthermore, it can be seen from Fig. 7 that the reduction gradually proceeds to a higher degree with increasing Ln-substitution level. One possible reason may be the structural stress induced by the substitution [19].

The question remains if the reduction of La_2RuO_5 remains incomplete because of kinetic or thermodynamic reasons. The formation of a partly reduced ruthenium oxide containing rare-earth ions cannot be excluded although no indications for such a phase were found in the EXAFS data. Especially in the case of a rare-earth-poor phase, the corresponding Ln-coordination spheres may well be hidden under the very intense Ru-related peaks in the mRDF. Therefore, the occurrence of (X-ray amorphous) suboxides during reduction has to be taken into account. On the other hand, it is remarkable that an incomplete reaction was only observed for (substituted) La_2RuO_5 while chemically related compounds like $(La,Sr)_2(Ru,Cu)O_{4-\delta}$ or $(La,Sr)_4RuO_{7+\delta}$ become completely reduced under the same conditions [5,7]. Kinetic reasons cannot be

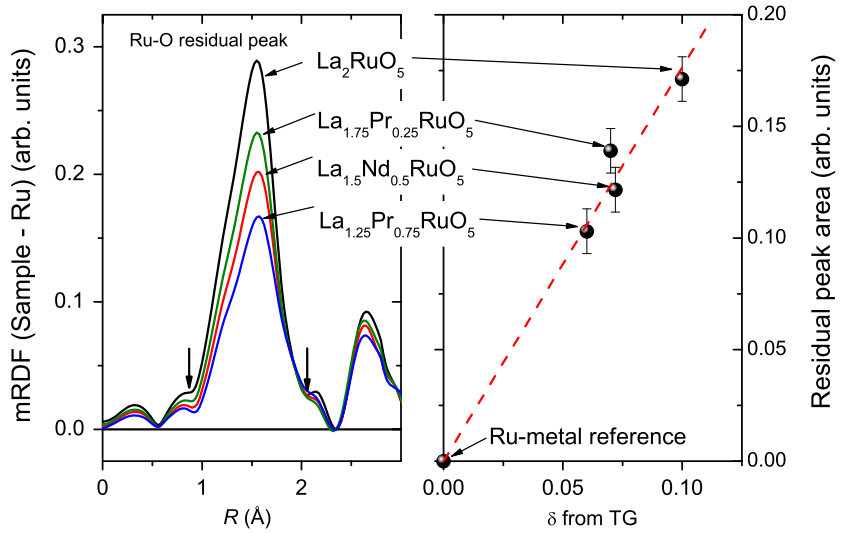

Fig. 7. Left: residuals of the Ru–K mRDF after subtraction of the fit of the first Ru-coordination shell. Right: residual peak area vs. oxygen deficiency obtained from TG measurements. The dashed line represents a linear regression.

excluded either. For example, the formation of a (again possibly La-containing) shell around an unreacted oxide core leading to a diffusion-controlled reaction rate seems plausible. Still the distinctively different reaction behavior of La_2RuO_5 compared to other rare-earth ruthenates is puzzling. Further investigations including longer reaction times and/or higher temperatures as well as HRTEM are planned to address these questions.

4. Summary and conclusions

The reduction of La_2RuO_5 and rare-earth substituted $La_{2-x}Ln_xRuO_5$ was studied by thermogravimetry to derive the exact oxygen stoichiometries of the compounds. For all samples a two-step reduction behavior was observed with the formation of a stable intermediate. Onset temperatures of the first reduction step were found to depend on the synthesis conditions. For all samples the observed total weight losses were significantly smaller than expected. Assuming complete reduction, the calculations lead to (apparent) oxygen deficiencies $0.06 \leq \delta \leq 0.14$ in clear contradiction to earlier results from neutron diffraction, XAS and magnetic measurements. The lack of XRD peaks corresponding to metallic ruthenium was a first hint pointing to an incomplete reaction.

XANES measurements show that the structure of the Ru–L_{III} absorption edge does not resemble the one of metallic ruthenium. On the contrary, the presence of a very intense white line indicates a Ru4*d*–O2*p* hybridization, i.e. the presence of oxygen. Ru–K EXAFS measurements clearly show the presence of Ru–O bonds and in turn an incomplete reduction of the transition metal. It was possible to quantify the amount of remaining oxygen and a linear correlation with the apparent oxygen deficiency of the samples was found. This linear relation proves that the calculated oxygen deficiencies are actually artifacts, resulting from an incomplete reaction even at temperatures up to 1100 °C.

This incomplete reduction of La_2RuO_5-type samples is an unusual exception, as all other ruthenium oxides we studied to date can readily be reduced.

In this paper we introduced an example for the failure of oxygen content determination by thermogravimetry although at first sight no problems were expected. The reduction of late (nobel) transition metal oxides usually leads to the corresponding metals and especially numerous ruthenium oxides have been successfully investigated by this method. Nevertheless, one must not forget that the determination of oxygen contents by thermogravimetry will only yield correct results if

a) the starting material is phase-pure and
b) the reduction products are well-defined.

As shown in this work, extra attention has to be paid to the latter restriction and hand-waving arguments ("What else could it be?") are clearly inappropriate.

Acknowledgments

The authors gratefully acknowledge HASYLAB for allocating beamtime and Edmund Welter for technical support.

References

[1] H.R. Oswald, A. Reller, Thermochim. Acta 95 (1985) 311–318.
[2] H.R. Oswald, A. Reller, J. Therm. Anal. 33 (1988) 67–74.
[3] W. Bensch, H.W. Schmalle, A. Reller, Solid State Ionics 43 (1990) 171–177.
[4] H.R. Oswald, S. Felder-Casagrande, A. Reller, Solid State Ionics 63–65 (1993) 565–569.
[5] S. Ebbinghaus, A. Reller, Solid State Ionics 101–103 (1997) 1369–1377.
[6] S. Ebbinghaus, M. Fröba, A. Reller, J. Phys. Chem. B 101 (1997) 9909–9915.
[7] T. Götzfried, A. Reller, S.G. Ebbinghaus, Solid State Sci. 6 (2004) 1205–1210.
[8] K. Wurr, A. Reller, J. Therm. Anal. 47 (1996) 339–348.
[9] F. Lichtenberg, D. Widmer, J.G. Bednorz, T. Williams, A. Reller, Z. Phys. B Condens. Matter. 82 (1991) 211–216.
[10] P. Boullay, D. Mercurio, A. Bencan, A. Meden, G. Drazic, M. Kosec, J. Solid State Chem. 170 (2003) 294–302.
[11] S.G. Ebbinghaus, Acta Crystallogr. Sect. C 61 (2005) i96–i98.
[12] P. Khalifah, R. Osborn, Q. Huang, H.W. Zandbergen, R. Jin, Y. Liu, D. Mandrus, R.J. Cava, Science 297 (2002) 2237–2240.
[13] S.K. Malik, D.C. Kundaliya, R.D. Kale, Solid State Commun. 135 (2005) 166–169.
[14] S. Riegg, A. Günther, H.-A. Krug von Nidda, A. Loidl, M.V. Eremin, A. Reller, S.G. Ebbinghaus, Phys. Rev. B 86 (2012) 115125.
[15] V. Eyert, S.G. Ebbinghaus, T. Kopp, Phys. Rev. Lett. 96 (2006) 256401.
[16] V. Eyert, S.G. Ebbinghaus, Prog. Solid State Chem. 35 (2007) 433–439.
[17] Hua Wu, Z. Hu, T. Burnus, J.D. Denlinger, P.G. Khalifah, D.G. Mandrus, L.-Y. Jang, H.H. Hsieh, A. Tanaka, K.S. Liang, J.W. Allen, R.J. Cava, D.I. Khomskii, L.H. Tjeng, Phys. Rev. Lett. 96 (2006) 256402.
[18] S.G. Ebbinghaus, S. Riegg, T. Götzfried, A. Reller, Eur. Phys. J. Spec. Top. 180 (2010) 91–116.
[19] S. Riegg, U. Sazama, M. Fröba, A. Reller, S.G. Ebbinghaus, Phys. Rev. B 84 (2011) 014403.
[20] S. Riegg, A. Günther, H.-A. Krug von Nidda, M.V. Eremin, A. Reller, A. Loidl, S.G. Ebbinghaus, Eur. Phys. J. B 85 (2012) 413.
[21] S. Riegg, A. Reller, S.G. Ebbinghaus, J. Solid State Chem. 188 (2012) 17–25.
[22] S. Riegg, S. Widmann, A. Günther, H.-A. Krug von Nidda, A. Reller, A. Loidl, S.G. Ebbinghaus, J. Phys. Condens. Matter 25 (2013) 126002.
[23] J.A. Bearden, A.F. Burr, Rev. Mod. Phys. 39 (1967) 125–142.
[24] K.V. Klementiev, J. Phys. D Appl. Phys. 34 (2001) 209–217.
[25] T. Ressler, J. Synch. Rad. 5 (1998) 118–122.
[26] A.L. Ankudinov, B. Ravel, J.J. Rehr, S.D. Conradson, Phys. Rev. B 58 (1998) 7565–7576.
[27] A. Benčan, M. Hrovat, J. Holc, G. Dražič, M. Kosec, J. Eur. Ceram. Soc. 25 (2005) 943–948.
[28] S.G. Ebbinghaus, Z. Hu, A. Reller, J. Solid State Chem. 156 (2001) 194–202.
[29] M.H. Aguirre, D. Logvinovich, L. Bocher, R. Robert, S.G. Ebbinghaus, A. Weidenkaff, Acta Mater. 57 (2009) 108–115.
[30] S.G. Ebbinghaus, J. Solid State Chem. 177 (2004) 817–823.
[31] S.G. Ebbinghaus, E.-W. Scheidt, T. Götzfried, Phys. Rev. B 75 (2007) 144414.
[32] T. Götzfried, A. Reller, S.G. Ebbinghaus, Inorg. Chem. 44 (2005) 6550–6557.